Green Photoinduced Modification of Natural Poly(3-hydroxybutyrate-*co*-3-hydroxyvalerate) Surface for Antibacterial Applications

G. M. Manecka,[†] J. Labrash,[†] O. Rouxel,[†] P. Dubot,[†] J. Lalevée,[‡] S. Abbad Andaloussi,[§] E. Renard,[†] V. Langlois,[†] and D. L. Versace*,[†]

[†]Institut de Chimie et des Matériaux Paris-Est, Equipe Systèmes Polymères Complexes, UMR 7182, CNRS-Université Paris-Est Créteil Val de Marne 2-8 rue Henri Dunant, 94320 Thiais, France

[‡]Institut de Science des Matériaux de Mulhouse, IS2M-LRC 7228, 15 rue Starcky, 68057 Mulhouse, France

[§]Unité Bioemco Equipe IBIOS, UMR 7618 CNRS-Université Paris-Est Créteil Val-de-Marne, 61, Avenue Général de Gaulle, 94010 Créteil cedex, France

ⓢ *Supporting Information*

ABSTRACT: A green photoinduced method for the modification of a biodegradable and biocompatible polymer, poly(3-hydroxybutyrate-*co*-3-hydroxyvalerate) (PHBHV), has been successfully carried out using three types of monomers with potential antibacterial effects, i.e., 2-[(methacryloyloxy)-ethyl] trimethylammonium chloride (META), 2-[(methacryloylethyl)]-dimethyl-(3-sulfopropyl) ammonium (MESA) and 2-hydroxyethyl methacrylate (HEMA). The photografting process is conducted through a photoinduced free radical process employing a ketone-based photoinitiator in an aqueous medium. Under appropriate conditions, the photogenerated radicals abstract hydrogen atoms from the PHBHV backbone, thus initiating the UV-mediated photopolymerization of derived-(meth)acrylate monomers from the surface of PHBHV film. The photochemical mechanism of the ketones photolysis is entirely described by a electron spin resonance/spin trapping technique, and the modified-PHBHV films are extensively characterized by ATR-FTIR and water contact angle and XPS measurements. Finally, a primary investigation is conducted to support the antibacterial activity of the new functionalized biomaterial against *Escherichia coli* and *Staphylococcus aureus*.

KEYWORDS: *Photochemistry, Poly(3-hydroxybutyrate-co-3-hydroxyvalerate), Photografting, Antibacterial activities*
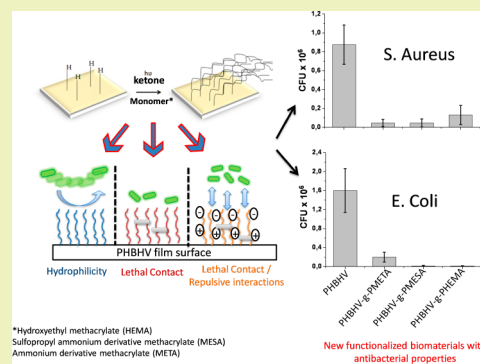
■ INTRODUCTION

Infection by pathogenic microorganisms is of great concern in the medical field particularly for medical devices, hospital surfaces/furniture, and surgery equipment. Infectious disease worldwide killed more people than any other disease and is responsible for the annual death of 100,000 people in the United States.[1,2] To solve the problem of increasing resistance of bacteria toward antibiotics, much attention has been paid on developing new antimicrobial systems in biomedical industry. Despite the potentially daunting complexity of bacteria populations and of materials surface characteristics, new chemical strategies have been developed to limit and prevent the bacterial colonization on material surfaces.

The first approach has focused on developing coatings that produce reactive radical species that have no specific target within bacteria upon light activation. Two main coating types were developed, i.e., photosensitizer-immobilized[3] and titanium dioxide-based photocatalyst coatings.[4−6] The second approach has involved biocide leaching, namely, use of antibiotics,[7] cytotoxic organic compounds,[8,9] inorganic compounds,[10−16]

metal nanoparticles,[17] or flavonoids,[18] which diffuse over time from a polymer materia, thus inducing death of adhered bacteria. Unfortunately, antimicrobial surface treatments erode quickly, which has serious adverse effects on the durability of the modified materials. Another serious issue with the use of leaching materials is that the released compounds increase drug resistance throughout the microbial realm and materials need to be regenerated to maintain their activities.
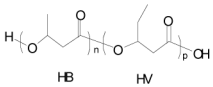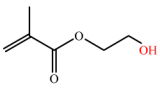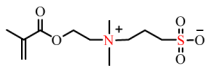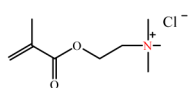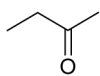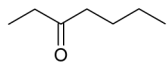
Covalently attaching antimicrobial systems to the surface presents an efficient alternative in the production of stable surface-active bactericidal materials. A number of active antimicrobial substances have been tested on various surfaces to address deficiencies in using leaching materials. Perfluorinated molecules[19] or polymers based on ethylene glycol[20,21] are the most widely used synthetic materials to reduce nonspecific protein adsorption. However, the oxidation of PEG units into

Table 1. Structure of Monomers/Polymer and Photoreactive Systems Used in This Study

Compounds	Function	Structure
Poly(3-hydroxybutyrate-*co*-3-hydroxyvalerate)	Polymer	
2-Hydroxyethyl methacrylate (HEMA)	Methacrylate monomer	
2-(Methacryloylethyl)-dimethyl-(3-sulfopropyl) ammonium (MESA)	Methacrylate monomer	
[2-(Methacryloyloxy)ethyl] trimethylammonium chloride (META).	Methacrylate monomer	
Butan-2-one	Photoinitiating system	
Heptan-3-one	Photoinitiating system	

reactive aldehyde moieties in the presence of transition metal ions and oxygen found in biologically relevant solutions[22,23] has forced the scientific community to design new strategies for creating novel, permanent, nonbiofouling, antibacterial surfaces. Recently, polymers including charged groups have gained attention as efficient bactericides. When positively charged molecules come into contact with bacteria, they can penetrate the cell membrane, disrupt its integrity, and provoke cell lysis. Several other types of polymers have been used: those that mimic natural peptides,[24,25] guanidine-containing polymers,[26,27] phospho- and sulfo-derivative-containing polymers,[28−31] phenol and benzoic acid derivative polymers,[32,33] organometallic polymers,[34] polyelectrolyte multilayers,[35] polymers with quaternary ammonium groups,[36−39] and zwitterionic polymers[40] such as poly(sulfobetaine methacrylate) or poly-(carboxybetaine methacrylate). The latter shows perhaps the greatest promise in the realm of surface-active compounds and has become the most popular synthetic polymer for developing nonbiofouling surfaces. Numerous investigations have described methods for treating surfaces such as using gold,[41] polyester surfaces,[42] polystyrene surfaces,[42] polyethylene slides,[43] silicon wafers,[44] titanium alloys,[45] HDPE,[46] LDPE,[46] nylon,[46] PP,[46] and PET.[46] Most of these studies used the ATRP method to graft functionalized polymers onto the material surface.[41,47]

To the best of our knowledge, no report has hitherto been published on the UV photografting of polymers with antibacterial properties from poly(3-hydroxyalkanoate)s (PHAs) films according to an environmentally substainable "green chemistry" method. In such an original approach,

polymers are expected to be located on the surface of PHBHV films in direct contact with bacteria for improving antibacterial activity.

Poly(3-hydroxyalkanoate)s (PHAs) constitute an enlarged family of biodegradable and biocompatible aliphatic polyesters[48−50] produced by many bacterial microorganisms when subjected to stress conditions. They can be considered as promising biopolymers and have attracted much interest for a variety of medical applications,[51−59] which include controlled drug release, fracture repair, bone and cartilage remolding, and tissue engineering in general. To enhance their properties, the direct surface modification of PHBHV films appears as a real challenge. Many physical or chemical modifications have been developed in order to tune PHAs film surface properties.[51,52,60−66] However, in order to preserve the integrity of the film, mild grafting conditions are required. To this end, photoinduced grafting represents a promising way to introduce functional groups on PHBHV surface. Indeed, this technique is widely known to be a useful "green method" for the functionalization of polymeric materials[67,68] due to its significant advantages, such as low cost of operation, innovative technology, and mild conditions. The photopolymerization process is a substrate-independent method allowing for the covalent deposition of a broad range of polymers. These technical aspects make photopolymerization a particularly useful method for surface modification strategies. Few studies have described so far the potentialities offered by the photoinduced graft polymerization method for the film surface modification of PHBHV. Its feasibility was essentially demonstrated through "grafting-from" polymerization with

997

dx.doi.org/10.1021/sc400564r | ACS Sustainable Chem. Eng. 2014, 2, 996−1006

the use of benzophenone,[69−71] a photosensitive system based on aryl azides,[72] hydrogen peroxide,[73] or triarylsulfonium salts.[66]

The novelty of the results presented in this paper lies in the development of a mild and simple method that uses an aqueous photoinitiating strategy to efficiently functionalize and tailor the surface properties of natural poly(3-hydroxybutyrate-*co*-3-hydroxyvalerate) films with polymers having antibacterial properties. A lack of existing research prompted us to examine more closely the effect of ketone photoinitiating systems on the modification of the surface of PHBHV films. The latter process is a one-step grafting process in water, and it is efficient enough to avoid homopolymerization of numerous monomers under light activation.

The first part of this study demonstrates the ability of two ketones to form radical species able to abstract hydrogen atoms from the surface of a PHBHV backbone using an electron spin resonance/spin trapping (ESR-ST) analysis. In the second part, a particular effort is made to demonstrate the photografting of poly(2-hydroxyethyl methacrylate), poly(2-(methacryloyloxy)-ethyl trimethylammonium), and poly(2-(methacryloylethyl)-dimethyl-(3-sulfopropyl) ammonium) from the PHBHV film surface. For this purpose, the grafted surfaces are characterized by X-ray photoelectron spectroscopy (XPS), Fourier transform infrared spectroscopy (ATR-FTIR), and gravimetric and water contact angle measurements. To validate the study, the antibacterial activity of modified PHBHV fibers against *Escherichia coli* (*E. coli*) and *Staphylococcus aureus* (*S. aureus*) is finally evaluated.

■ EXPERIMENTAL SECTION

Materials. Poly(3-hydroxybutyrate-*co*-3-hydroxyvalerate) (PHBHV) with 12% of 3-hydroxyvalerate (HV) and a molar mass of 90,000 g/mol was purchased from GoodFellow. PHBHV was first purified by dissolution in chloroform for 2 h (10% w/v) and precipitated in ethanol for removing citric ester used as plasticizer. 2-Hydroxyethyl methacrylate (97%, HEMA), 2-(methacryloyloxy)-ethyl trimethylammonium (80%, META), and 2-(methacryloylethyl)-dimethyl-(3-sulfopropyl) ammonium (97%, MESA) were purchased from Sigma-Aldrich. Butan-2-one (99%) and heptan-3-one (98%) was provided from Alfa-Aesar. Methylene chloride (CH_2Cl_2) and ethanol were supplied by Carlo Erba. All of the aqueous solutions were prepared using ultrapure water. The structures of the respective polymers and the photoinitiating systems are shown in Table 1.

Preparation of PHBHV Films. To get rid of the plasticizer (citric acid), PHBHV granules (20 g) were dissolved in 200 mL of methylene chloride and stirred at 50 °C until the solution became completely homogeneous. The solution was then precipitated in ethanol solution (1.5 L). The pure PHBHV was obtained after filtration and dried under vacuum at room temperature during one night. Pure PHBHV powder was placed between two Teflon films and baked at 160 °C for 5 min under pressure of 2 bar. Films with a thickness of 30 μm were obtained and cut into pieces 1.5 cm × 1.5 cm.

Photografting Procedures. A total of 300 μL of a suitable concentration of the selected monomer solution in distilled water (containing butan-2-one or heptan-3-one as a photoinitiating system) was added by a micropipet on the surface of the PHBHV film. The thin and uniform liquid layer was sandwiched between a PHBHV support and a polypropylene film, which is transparent to UV light. Polypropylene film was used to hinder oxygen diffusion inside photopolymerized solution. Both sides of the PHBHV film/monomer/polypropylene film assembly were irradiated at room temperature by means of a Lightningcure LC8 (L8251) from Hamamatsu equipped with a mercury−xenon lamp (200 W) coupled with a flexible light guide. The end of the guide was placed at a distance of 11 cm. The maximum UV light intensity at the sample

position was measured by radiometry (International Light Technologies ILT 393) to be 180 mW/cm^2 in the 250−450 nm. Photografted PHBHV films were then put into distilled water overnight and allowed to dry for one day before characterization. The extent of grafting (*G*) was calculated in mg cm^{-2}, using eq 1

$$G = \frac{W_g - W_o}{S} \tag{1}$$

where W_g is the weight of the film after grafting, W_o the initial weight of the film, and *S* is the surface of the films.

Attenuated Total Reflection-FTIR (ATR-FTIR) Spectroscopy. The FTIR spectra of PHBHV and PHBHV-modified films were recorded with a Bruker Tensor 27 spectrophotometer equipped with an attenuated internal reflection accessory using a diamond crystal. Infrared spectra were collected at a resolution of 4 cm^{-1} with an accumulation of 32 scans. For the Fourier transformation of the interferogram, a Blackman-Harris-3-term apodization function was selected as well as a zero-filling factor of 2 and a standard Mertz procedure for phase correction.

X-ray Photoelectron (XPS). X-ray photoelectron (XPS) measurements, at a mean takeoff angle of 20°, were performed with a Mac2RIBER with a resolution of 1 eV. Survey scans were done using a monochromatic Mg Kα X-ray source (12 KeV, 2 mA) with a spot diameter of 25 mm^2 operated in a low power mode (24 W) to avoid degradation and chemical modification induced by irradiation. A pass energy of 10 eV was used for the detailed XPS scans. XPS spectra were obtained with an energy step of 0.05 eV with a dwell time of 200 ms. Data acquisitions have mainly been focused on the C1s, O1s, N1s, and S2s (and S2p$_{3/2}$) core level lines. The elemental composition as well as element chemical bonding can be deduced from peak shapes as binding energy of the atomic orbital is strongly influenced by local potential of the emitting atom (initial state effect). In our study, a maximum of four peaks for C1s, three peaks for O1s, and one peak for N1s and S2s (or S2p$_{3/2}$) are used for band deconvolution; each one corresponding to a specific local chemical environment. The C1s and O1s envelopes were analyzed and peak-fitted using Gaussian line shapes (with the ORIGIN software) with a mean value of the full width at half-maximum (fwhm) of 1.8 eV for C1s core level lines, while 2.0 eV for O1s. Full width at half maximum (fwhm) was constrained for a given core level line with different chemical environments during peak fitting processing, and the inelastic electron backgrounds have been removed using the Shirley method. The binding energy scale was fixed by assigning a binding energy of 285.1 eV to the −CH− carbon (1s) peak.

Electron Spin Resonance/Spin Trapping (ESR-ST). Electron spin resonance/spin trapping (ESR-ST) experiments were carried out using an X-band spectrometer (Bruker EMX-plus Biospin). The radicals were generated under argon at room temperature using a polychromatic light irradiation (Xe−Hg lamp; Hamamatsu, L8252, 150 W) and trapped by phenyl-N-tertbutylnitrone (PBN). The ESR spectra simulations were done with the PEST WINSIM program. All of the samples were prepared in a 6 mm quartz cylindrical tube and dissolved in *tert*-butylbenzene as an inert solvent.

Static Contact Angle Measurements. The water contact angle was measured using standard methods. In all the experiments described in this study, static contact angles were measured using a goniometer from Krüss (Easy Drop Krüss). The first step of the measurement was to place a water drop of defined volume on the film surface, which was always exactly horizontal. To apply reproducible uniform volume drops of deionized water, calibrated micropipets were used; in general, the volume of the water drop was in the range of 15−20 μL. Drop shape was automatically recorded with a high speed framing camera; images were then processed by a computer and stored. The uncertainty in the measurements depends on the light−dark contrasts of the drop picture, and an error of 3−4° could be assumed.

Antibacterial Activity. (i) Two strains of bacteria were used, *S. aureus* ATCC6538 and *E. coli* ATCC25922. Prior to in vitro antibacterial tests, the bacterial strains were grown aerobically
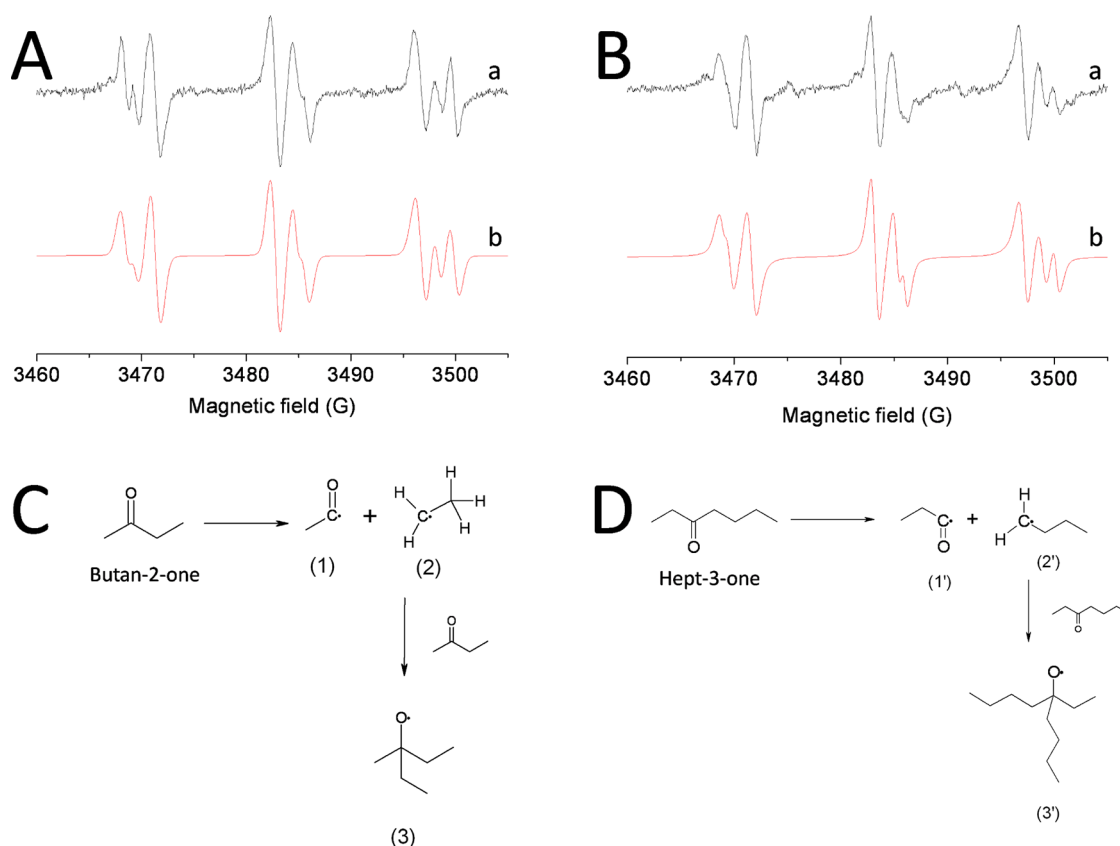
Figure 1. ESR-ST signals of butan-2-one (A) and heptan-3-one (B) after 30 s of irradiation with a Hg–Xe lamp: (a) Experimental and (b) simulated data. Solution is degassed with argon for 5 min. Radicals are trapped by PBN. Experiments were done at room temperature. Mechanistic approaches to butan-2-one (C) and heptan-3-one (D) photolysis after 30 s of irradiation. Radicals are trapped by PBN.

overnight on Müller–Hinton medium at 37 °C under stirring. (ii) Evaluation of the bacterial adherence on the PHBHV and the modified PHBHV-based films was performed as follows: the films were immersed in a bacterial solution ($OD_{600\ nm}$ = 0.05) for 1 h; then, nonadherent bacteria on the sample surface were removed by washing several times with sterilized water before incubation of the films in a neutral medium. After 24 h of incubation at 37 °C, the materials were submitted to a vortex and ultrasound in physiological saline buffer to remove any adherent bacteria from the surface. A 100 μL volume of the detached viable bacteria solution was introduced onto the surface of a Müller–Hinton-type agar plate. Finally, the total bacterial adherence was determined by a counting of the CFUs, after overnight incubation of the agar plates at 37 °C, for all cultivated bacteria strains.

Statistical Analysis. All values corresponding to the anti-adherence activity of *S. aureus* and *E. coli* are expressed as mean ± standard deviation. Statistical analysis was performed using the Student's *t*-test for the calculation of the significance level of the data. Differences were considered statistically significant at $P < 0.05$. Ten samples per group were evaluated.

■ RESULTS AND DISCUSSION

The first step of our methodology concerns the bottom-up growth of different polymers tethered chains from the PHBHV film surface according to a photoinduced free radical method. The different stages of the free radical reaction are presented hereafter.

Photolysis of Ketones Under UV Irradiation. Ketones were used because of its solubility in water, and few investigations related to their reactivity under light activation have been described so far. The ability of two kind of ketones to generate efficient radicals in the "grafting-from" process was described using ESR/ST. Figure 1A and B display the ESR-ST

signals of, respectively, butan-2-one and heptan-3-one upon Xe–Hg lamp UV irradiation (200−400 nm) under argon saturated solution. Figure 1A and B provide spectra that consist of a mixture of two radical species derived both from carbon-centered and oxygen-centered radicals. It should be pointed out that the experimental data (Figure 1A-a and B-a) are in excellent agreement with the simulated results (Figure 1A-b and B-b). The corresponding hyperfine coupling constant values of these radicals are summarized in Table 2. The first

Table 2. Hyperfine Coupling Constant Values of Radical Spin Adducts with PBN after 30 s of Irradiation of Butan-2-one and Heptan-3-one[a]

compound	carbon-centered radical			oxygen-centered radical		
	a_N (G)	a_H (G)	(%)	a_N (G)	a_H (G)	(%)
butan-2-one	14.2	3	47	13.5	1.8	53
heptan-3-one	14.2	3	20	13.7	1.9	80

[a]The light intensity is 180 mW cm^{-2}. Solution is degassed with argon for 5 min.

PBN radical adduct with the parameters of a_N = 14.2G and a_H = 3G (or a_N = 14.2G and a_H = 3G) can be confidently assigned to a carbon-centered radical: an acyl radical,[74] namely, $CH_3C(=O)\bullet$ (Figure 1C-1) or $C_2H_5C(=O)\bullet$ (Figure 1D-1'), resulting from the homolytic $CH_3C(=O)-C_2H_5$ or $C_2H_5C(=O)-C_4H_9$ single bond photocleavage, respectively, as described in Figure 1C and D, respectively.

The hyperfine coupling constants of the second radical produced from butan-2-one (a_N = 13.5G; a_H = 1.8G) or

heptan-3-one (a_N = 13.7G; a_H = 1.9G) are fully consistent with those of an oxygen-centered radical. The global mechanisms of the ketone photolysis are thus described in Figure 1C and D. Alkyl radicals (Figure 1C-(2) or D-(2′)) are capable of being added to the carbonyl group of ketones to generate alkoxy adduct radicals[75] (Figure 1C-(3) or D-(3′)).

Photochemical Modification of PHBHV Films Under Light Activation. In most of the studies done in UV photografting, benzophenone and its derivatives have been used as photoinitiating systems.[69−71] However, such compounds are only solubilized into organic solvents. The photografting investigation in this study will be performed in accordance with a "green chemistry" procedure with the use of water-soluble photoinitiators, i.e., butan-2-one and heptan-3-one.

As a preliminary step, grafting process of HEMA, META, or MESA monomers with two ketone photoinitiating systems without UV irradiation was assessed by FTIR-ATR. Any sign of modification was detected over one week, thus confirming the absence of grafting without UV irradiation. The second time it was also checked that PHBHV films were not modified under UV irradiation. Prior to photografting, 300 μL of an aqueous monomer solution containing a ketone as a photoinitiating system was added by a micropipet on the surface of the film, forming a thin and uniform liquid layer. In the second step, samples were irradiated with an intensity of 180mW/cm², leading either to a coloration change with HEMA or a transparent layer with META or MESA. In this study, butan-2-one or heptan-3-one were used for activating the PHBHV surface according a "grafting-from" technique. Scheme 1 outlines the photografting of an acrylate-derived monomer onto PHBHV film using a ketone system. The photolysis ((1), Scheme 1) of the latter generates both a carbon radical (A) and an alkoxy adduct radical (B), which are capable of hydrogen abstraction. The latter diffuse to the aqueous monomer solution to abstract a hydrogen atom from the PHBHV surface ((2),
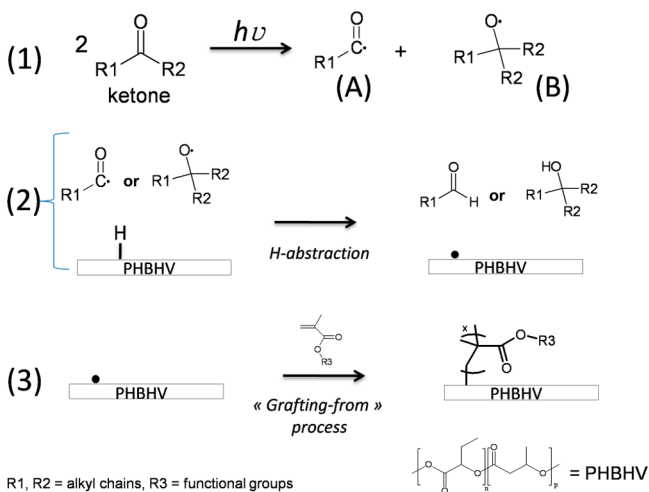
Scheme 1). The hydrogen atom in the β position of −COO ester groups in PHBHV is likely to be the more labile atom toward hydrogen abstraction. Nevertheless, the hydrogen atoms in the α position with respect to carbonyl groups can potentially be abstracted as well. The latter reaction generates free radicals onto the PHBHV surface that initiate the polymerization of an acrylate monomer, thus producing surface-grafted acrylate chains ((3), Scheme 1).

The ATR-FTIR spectrum of the PHBHV sample (Figure 2A) shows typical absorption bands, namely, −C−H aliphatic
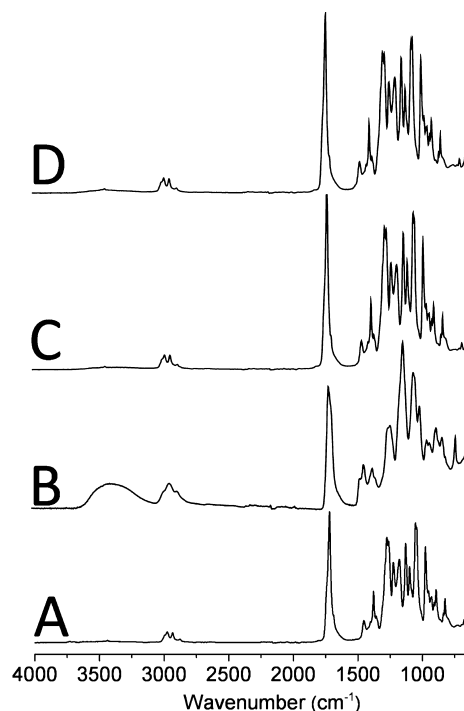

Figure 2. ATR-FTIR spectra of photomodified PHBHV films. (A) Native PHBHV, (B) PHBHV-g-PHEMA film, (C) PHBHV-g-PMETA film, and (D) PHBHV-g-PMESA film.

and asymmetric stretching bands at 2870−3010 cm⁻¹ and a C=O stretching band at 1720 cm⁻¹ (ester group). In the HEMA-derived PHBHV sample (Figure 2B), the broad band from 3050 to 3600 cm⁻¹ is assigned to the O−H stretch of the alcohol, whereas an additional band is visible at 1700 cm⁻¹ and corresponds to the C=O stretch vibration of the HEMA. The acrylate double bonds (of HEMA) at 1636 cm⁻¹ disappears, while HEMA is polymerized. Indeed, the acrylate double bonds are consumed by the free radical polymerization reaction. This is evidence that the photopolymerization of HEMA occurs onto the surface of the PHBHV film. In the ammonium (META) and sulfopropyl ammonium (MESA) acrylate-modified PHBHV films (Figure 2C and D), the characterized acrylate band at 1636 cm⁻¹ also disappears, which demonstrates the efficiency of the photografting process. For both samples, the appearance of a weak additional band between 3200 and 3500 cm⁻¹ indicates the presence of an ammonium group at the PHBHV surface. ATR-FTIR spectra of HEMA, MESA, and META monomers and the corresponding modified PHBHV films in the range of 1600−1900 cm⁻¹ are displayed in the Supporting Information part to appreciate the disappearance of the acrylate double bonds after the irradiation.

Scheme 1. Mechanism of Acrylate Photografting from the Surface of PHBHV Films, According to a "Grafting-from" Process[a]

[a] (1) Photolysis of a ketone and production of both alkyl and alkoxy radicals. (2) Hydrogen abstraction from the PHBHV surface and generation of free radicals on the surface of the PHBHV films. (3) Free radicals initiate polymerization of an acrylate monomer from the PHBHV surface.
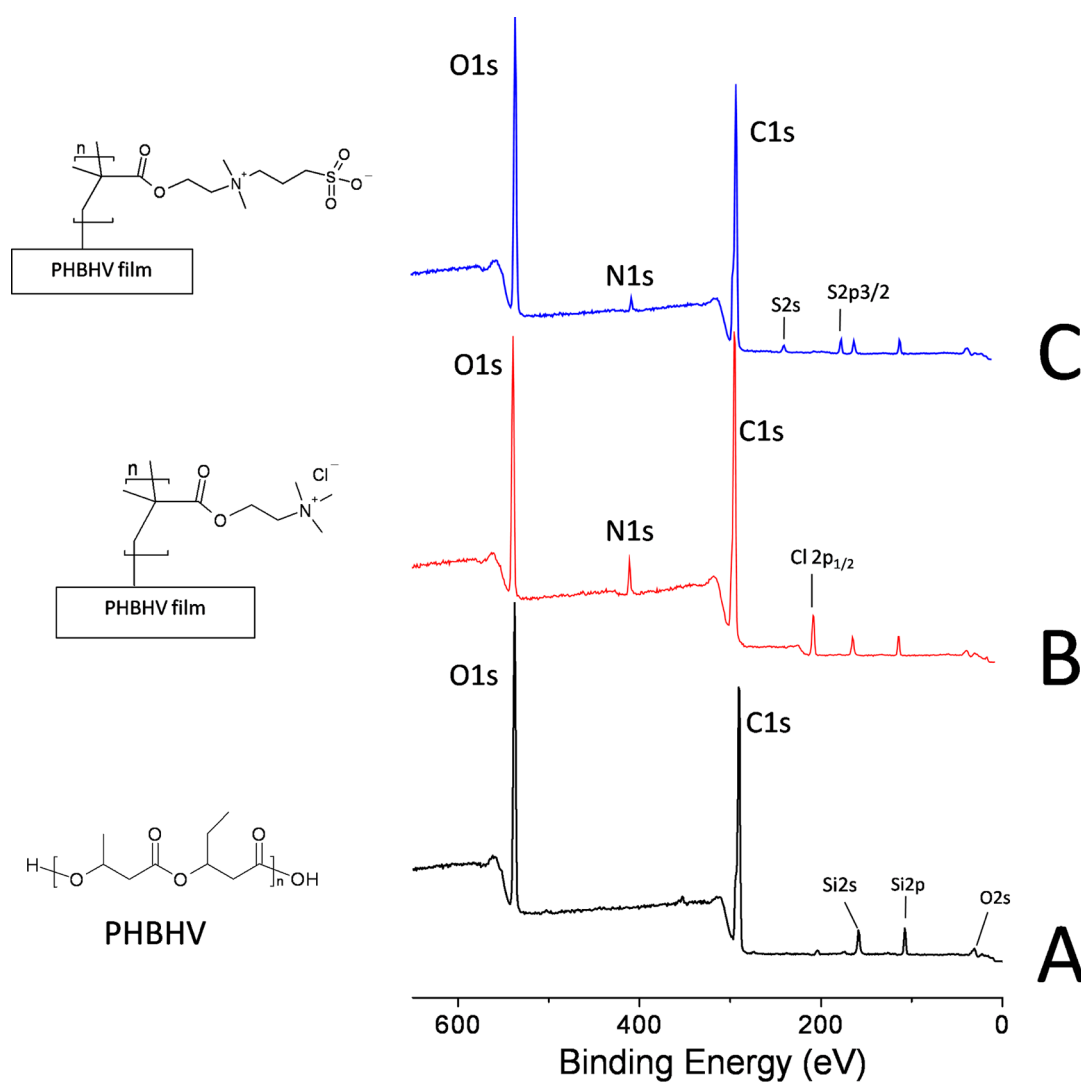
Figure 3. XPS survey-scan spectra of (A) PHBHV film, (B) PHBHV-*g*-PMETA film ([META] = 3M, butan-2-one/water/ethanol volume ratio: 10/10/10), and (C) PHBHV-*g*-PMESA film ([MESA] = 1M, butan-2-one/water/ethanol volume ratio: 10/10/10). Irradiation time = 300 s. Light intensity = 180 mW cm^{-2}; Hg–Xe lamp.

In order to investigate the chemical changes of PHBHV surfaces, XPS measurements have been performed using the Mg Kα X-ray source operated in a low power mode (24 W) to avoid degradation and chemical modification induced by irradiation. Data acquisitions have mainly been focused on the C1s, S2s, S2p$_{3/2}$, N1s, and O1s core level lines. The elemental composition as well as the element chemical bonding can be deduced from peak shapes as binding energy of the atomic orbital is strongly influenced by the local potential of the emitting atom. In our study, a maximum of four peaks for C1s (one peak for S2s (or S2p$_{3/2}$) and N1s) are used for band deconvolution, each one corresponding to a specific local chemical environment. XPS survey-scan spectra for unmodified PHBHV film and PHBHV-modified films with META and MESA are displayed in Figure 3. The XPS high resolution spectra of N1s and S2s (and S2p$_{3/2}$) regions of the PHBHV-*g*-PMETA and PHBHV-*g*-PMESA films are more specifically described in Figure 4. XPS assignment for the C1s, N1s, S2s, S2p$_{3/2}$, and O1s detailed spectra can be deconvoluted into four maximum main components as described in Table 3.

For nonmodified PHBHV film, the C1s spectrum demonstrates the appearance of three main components, aliphatic

carbon (C−H/C−C) at 285.1 eV, C−O bond at 286.7 eV, and carbon from carbonyl group (O−C=O) at 289.2 eV in good agreement with the literature[18]. The O1s spectrum is divided into two peaks: 532.1 and 533.4 eV for O−C=O and O−-C=O bonds, respectively.

In the case of PHBHV films modified with META (Figure 3B), the C1s core-level spectrum show four peak components with binding energies at 285.1, 286.1, 286.8, and 289.2 eV, which are attributed to C−H/C−C, C−N$^+$, C−O, and O−C=O, respectively. For the same sample, the binding energy of the N1s core level of the ammonium group (C−N$^+$) is located at 403.1 eV (Figures 3B and 4A).

Concerning the PHBHV-*g*-PMESA film (Figure 3C), two new peaks appear at 231.7 and 168.1 eV, respectively, for the S2s (Figure 4C) and S2p$_{3/2}$ (Figure 4D) core level of the sulfopropyl group. The N1s core level of the ammonium group (C−N$^+$) remains located at 403.1 eV (Figures 3C and 4B).

Figures 5A−D show the photografting of HEMA, META, and MESA onto PHBHV films carried out on different concentrations and ketones/water/ethanol ratios. According to Figure 5A, the extent of HEMA photografting with butan-2-one appears more efficient with an increase in water content
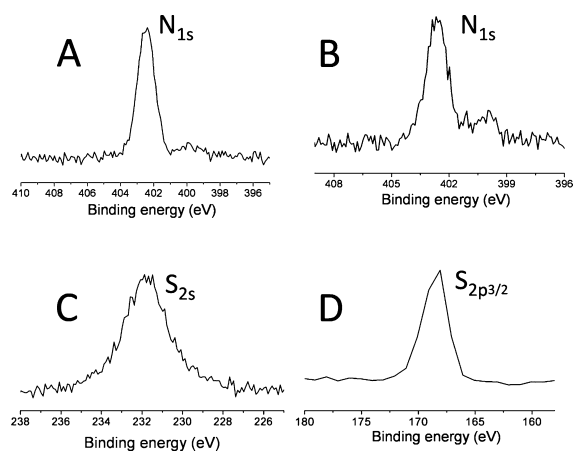
Figure 4. XPS high resolution spectra of the (A) N1s region of the PHBHV-*g*-PMETA film ([META] = 3M, butan-2-one/water/ethanol volume ratio: 10/10/10), B) N1s region of PHBHV-*g*-PMESA film, C) S2s region of the PHBHV-*g*-PMESA film and D) S2p$_{3/2}$ region of the PHBHV-*g*-PMESA film. Irradiation time =300 s, light intensity =180 mW.cm^{-2}, Hg−Xe lamp. [MESA] = 1 M with butan-2-one/water/ethanol volume ratio: 10/10/10.

(10/80/0 or 10/80/10 ratios). However, for these two ratios, the grafting of HEMA initiated by heptan-3-one failed. The efficiency of the photografting only occurs with an increase in ethanol ratio in the mixed solvents (10/40/50, Figure 5A). One possible reason for this difference is the low solubility of heptan-3-one in water, and the longer the alkyl chain is of the aliphatic ketone, the more ethanol is needed.[76] In the light of these results, it should be pointed out that butan-2-one is much more efficient than heptan-3-one for promoting the polymerization of acrylate monomers from the PHBHV surface. This observation is similar to that observed for the photografting of META (Figure 5C) or MESA (Figure 5D). Indeed, for the same volume ratio (10/10/10; ketone/water/ethanol), the extent of META grafting is higher with butan-2-one than heptan-3-one, but MESA has not lead to any successful grafting with heptan-3-one.

It should be also underlined that the concentration of acrylate monomers appears as a key factor for the surface modification of PHBHV films. As their reactivity differs from each other, the optimal concentration for each monomer has been adjusted to get the highest extent of grafting. As expected for the photografting of HEMA, an increase in monomer concentration from 1 to 4 M leads to a rise in the extent of grafting (Figure 5B). However, its significant augmentation to 8 M favors the homopolymerization and decreases the efficiency of the "grafting-from" process. As a matter of fact, the concentrations of META and MESA have been reduced to 3 and 1 M, respectively (Figures 5C and D). It should be interesting to point out that for an increase in the irradiation

time (>300s), the homopolymerization of 2-(methacryloylethyl)-dimethyl-(3-sulfopropyl) ammonium (MESA) occurs, thus preventing an appropriate cleaning and rinsing of the PHBHV-*g*-PMESA films that crack.

The reaction of the most effective ketone photoinitiating system (butan-2-one) with PHBHV films under UV irradiation in the presence of HEMA, META, or MESA was monitored by water contact angle measurements. The water contact angle is expected to drop significantly when PHBHV films are treated with the three types of monomers due to the hydrophilic nature of the hydroxyl, ammonium, and sulfopropyl ammonium groups that are grafted on the PHBHV surface. Figure 6 displays the evolution of the measured contact angle as a function of irradiation time. For the photografting of all the monomers, the water contact angle decreases as the exposure time is increased. After 300s of irradiation, the water contact angle decreases to 30°, 50°, and 75° for PHBHV-*g*-PMETA film, PHBHV-*g*-PHEMA film, and PHBHV-*g*-PMESA film, respectively. According to Figure 5, the longer the irradiation is, the higher the extent of grafting for each monomer is. A high concentration of hydrophilic functions (quaternary ammonium, hydroxyl or sulfopropyl groups) is expected at the surface of the modified PHBHV films for each monomer, thus decreasing the water contact angle of the corresponding films with the irradiation time. Finally, these results point out both the UV photografting of the three types of monomers onto the PHBHV film and the capability to tailor the surface hydrophilicity of the PHBHV films with the irradiation time.

Antibacterial Activity. The antibacterial activity of some polymers proved to be of great interest for the prevention of adhesion and proliferation activities of bacteria on material surfaces.[35] Therefore, the ability of the PHBHV-modified surface (with HEMA, MESA, and META) to inhibit the bacterial adhesion was evaluated with Gram-positive *Staphylococcus aureus* (*S. aureus*) and Gram-negative *Escherichia coli* (*E. coli*). Figure 7 summarizes the results of the antibacterial tests performed on PHBHV, PHBHV-*g*-PMETA, PHBHV-*g*-PMESA, and PHBHV-*g*-PHEMA films.

PHBHV film did not exhibit antibacterial activity which neither significantly inhibited (*P* > 0.05) the *S. aureus* nor affected the *E. coli* adherences. In contrast, the introduction of ammonium, sulfopropyl ammonium, and alcohol groups onto the PHBHV-based film surface led to a drastic inhibition of the bacterial adhesion of *S. aureus* and *E. coli*. Such PHBHV-derived materials with MESA and HEMA led to a reduction by 99% of the adherence of *Escherichia coli*. Results suggest that zwitterionic PHBHV-*g*-PMESA and PHBHV-*g*-PHEMA films are effective nonbiofouling materials to provide anti-adherence against *E. coli*. For PHBHV grafted with ammonium polyacrylate (PMETA), the adhesion is reduced by 90% compared to the nonmodified PHBHV film. This latter result is in accordance with some antibacterial investigations;[77,78] it is

Table 3. XPS Assignment for Unmodified PHBHV Film, PHBHV-*g*-PHEMA Film, PHBHV-*g*-PMETA Film, and PHBHV-*g*-PMESA Film

| nature of the film | C1s | | | | O1s | | | | N1s | S2s | S2p$_{3/2}$ |
	C−C/C−H	C−O	O−C=O	C−N$^+$	O*−C=O	O−C=O*	C−O*H	O*=S	N$^+$−C	RSO$_3^-$	RSO$_3^-$
PHBHV	285.1	286.7	289.2	−	532.1	533.4	−	−	−	−	−
PHBHV-*g*-PHEMA	285.1	286.7	289.4	−	531.9	533.6	532.5	−	−	−	−
PHBHV-*g*-PMETA	285.1	286.8	289.2	286.1	532.1	533.6	−	−	403.1	−	−
PHBHV-*g*-PMESA	285.1	286.8	289.2	285.9	532.2	533.5	−	531.2	403.1	231.7	168.1

1002

dx.doi.org/10.1021/sc400564r | *ACS Sustainable Chem. Eng.* 2014, 2, 996−1006
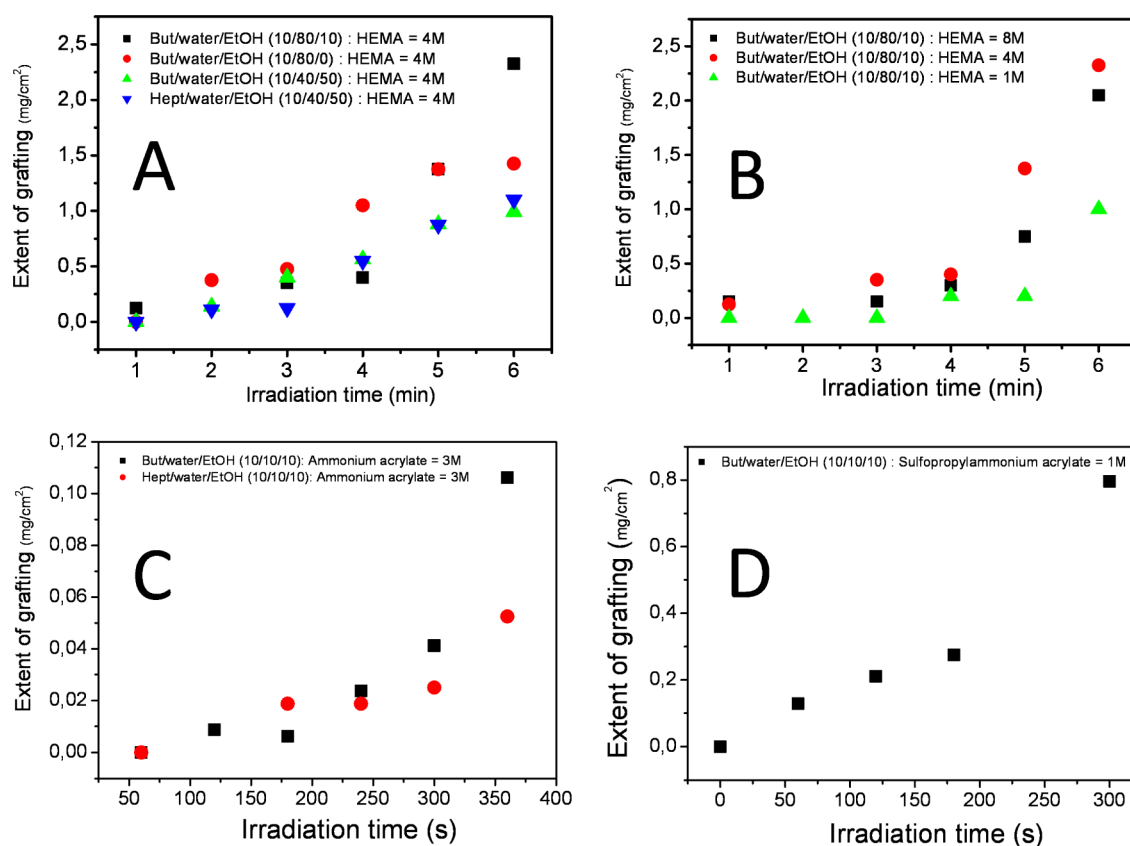
Figure 5. Effect of the irradiation time, nature of both monomers, and photoinitiating systems on the extent of grafting on PHBHV films. (A) Photografting reaction of an aqueous solution of HEMA (4 M) onto PHBHV film according to the nature of ketone and different volume ratios (ketone/water/EtOH). (B) Concentration effect of an aqueous solution of HEMA (with butan-2-one/water/EtOH: 10/80/10 v/v/v). (C) Photografting reaction of an aqueous solution of META (3 M) onto PHBHV film according to the nature of ketone (ketone/water/EtOH: 10/10/10 v/v/v). (D) Photografting reaction of an aqueous solution of MESA (1 M) onto PHBHV film with butan-2-one/water/EtOH: 10/10/10 v/v/v. Light intensity = 180 mW/cm^2; Hg−Xe lamp.
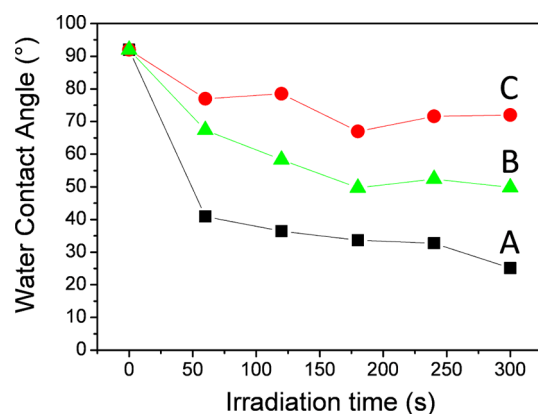

Figure 6. Evolution of the water contact angle of the modified PHBHV films for different irradiation times. (A) PHBHV-*g*-PMETA film ([META] = 3M, butan-2-one/water/ethanol volume ratio: 10/10/10), (B) PHBHV-*g*-PHEMA film ([HEMA] = 4M, butan-2-one/water/ethanol volume ratio: 10/80/10), and (C) PHBHV-*g*-PMESA film ([MESA] = 1 M with butan-2-one/water/ethanol volume ratio: 10/10/10).

generally assumed that the antibacterial activity against *E. coli* of copolymers containing quaternary ammonium groups is less efficient as the hydrophilic content of the polymers is increased.[79] With a contact angle of 30°, the anti-adherence (against *E. coli*) of PHBHV-*g*-PMETA film appears less

important than both PHBHV-*g*-PMESA and PHBHV-*g*-PHEMA films.

Results concerning *S. aureus* are similar whatever the polymer grafted onto PHBHV surface; an average reduction of around 90% for the anti-adhesion of *S. aureus* was demonstrated. These results underline that the hydrophilicity of the modified PHBHV films do not play a key role in the adhesion of *S. aureus*.

CONCLUSIONS

PHBHV-derived polymer films with antibacterial activity were successfully engineered according to an environmentally sustainable "green chemistry" approach. Our study has demonstrated an efficient green photografting method for the covalent surface modification of PHBHV films with three types of acrylate monomers under light activation and in aqueous media. Under UV irradiation, ketones afford the abstraction of a H atom from the PHBHV backbone, thus generating radicals that are able to initiate the radical polymerization of acrylate monomers according to a "grafting-from" process.

Such PHBHV-derived materials led to a tremendous inhibition of the adhesion of *Staphylococcus aureus* and a reduction by 99% of the adherence of *Escherichia coli*. This new route of grafting could be further used to broaden the application portfolio of PHAs. The possible uses of a permanent nonbiofouling surface such as described in this
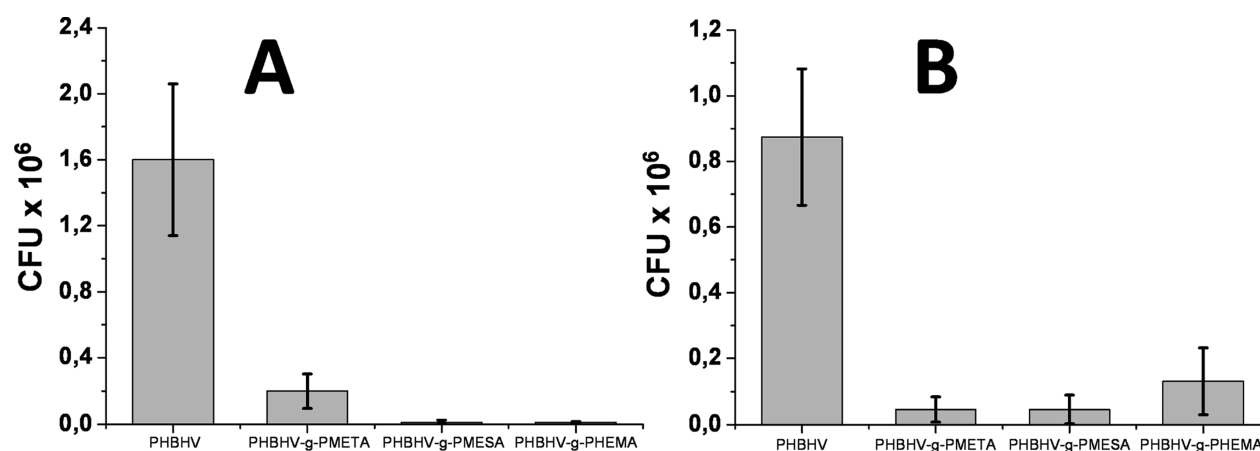
1003

dx.doi.org/10.1021/sc400564r | *ACS Sustainable Chem. Eng.* 2014, 2, 996−1006

Figure 7. Comparison of anti-adherence activity against *E. coli* (A) and *S. aureus* (B) of PHBHV, PHBHV-*g*-PMETA, PHBHV-*g*-PMESA, and PHBHV-*g*-PHEMA films. Data is shown as mean + standard deviation, $n = 10$. Results indicate significant difference obtained by *t* test ($P < 0.05$).

investigation would include, for example, treatment of food packaging or coating for biomedical devices.

ASSOCIATED CONTENT

Ⓢ Supporting Information

ATR-FTIR spectra of HEMA, MESA, META monomers, and the corresponding modified PHBHV films in the range of 1600−1900 cm^{-1}. This material is available free of charge via the Internet at http://pubs.acs.org.

AUTHOR INFORMATION

Corresponding Author
*E-mail: versace@icmpe.cnrs.fr. Tel: +33 1 49 78 12 28. Fax: +33 1 49 78 12 01.

Notes
The authors declare no competing financial interest.

ACKNOWLEDGMENTS

REFERENCES

(1) Klevens, R. M.; Edwards, J. R.; Richards, J. C. L.; Horan, T. C.; Gaynes, R. P.; Pollock, D. A.; Cardo, D. M. Estimating health care-associated infections and deaths in U.S. hospitals, 2002. *Public Health Rep.* **2007**, *122* (2), 160−166.

(2) Sampredo, M. F.; Patel, R. Infections associated with long-term prosthetic devices. *Infect. Dis. Clin. North Am.* **2007**, *21* (3), 785−819.

(3) Lim, K. S.; Oh, K. W.; Kim, S. H. Antimicrobial activity of organic photosensitizers embedded in electrospun nylon 6 nanofibers. *Polym. Int.* **2012**, *61* (10), 1519−1524.

(4) Perni, S.; Piccirillo, C.; Pratten, J.; Prokopovich, P.; Chrzanowski, W.; Parkin, I. P.; Wilson, M. The antimicrobial properties of light-activated polymers containing methylene blue and gold nanoparticles. *Biomaterials* **2009**, *30* (1), 89−93.

(5) Decraene, V.; Pratten, J.; Wilson, M. Cellulose acetate containing toluidine blue and rose bengal is an effective antimicrobial coating when exposed to white light. *Appl. Environ. Microbiol.* **2006**, *72* (6), 4436−4439.

(6) Matsunaga, T.; Tomoda, R.; Nakajima, T.; Nakamura, N.; Komine, T. Continuous-sterilization system that uses photosemiconductor powders. *Appl. Environ. Microbiol.* **1988**, *54* (6), 1330−1333.

(7) Ruckh, T. T.; Oldinski, R. A.; Carroll, D. A.; Mikhova, K.; Bryers, J. D.; Popat, K. C. Antimicrobial effects of nanofiber poly-(caprolactone) tissue scaffolds releasing rifampicin. *J. Mater. Sci: Mater. Med.* **2012**, *23* (6), 1411−1420.

(8) Lu, J.; Hill, M. A.; Hood, M.; Greeson, J. D. F.; Horton, J. R.; Orndorff, P. E.; Herndon, A. S.; Tonelli, A. E. Formation of antibiotic, biodegradable polymers by processing with Irgasan DP300R (triclosan) and its inclusion compound with *β*-cyclodextrin. *J. Appl. Polym. Sci.* **2001**, *82* (2), 300−309.

(9) Chung, D.; Papadakis, S. E.; Yam, K. L. Evaluation of a polymer coating containing triclosan as the antimicrobial layer for packaging materials. *Int. J. Food Sci. Technol.* **2003**, *38* (2), 165−169.

(10) Knetsch, M. L. W.; Koole, L. H. New strategies in the development of antimicrobial coatings: The example of increasing usage of silver and silver nanoparticles. *Polymers* **2011**, *3* (1), 340−366.

(11) Amna, T.; Hassan, M. S.; Barakat, N. A. M.; Pandeya, D. R.; Hong, S. T.; Khil, M.-S.; Kim, H. Y. Antibacterial activity and interaction mechanism of electrospun zinc-doped titania nanofibers. *Appl. Microbiol. Biotechnol.* **2012**, *93*, 743−751.

(12) Amarjargal, A.; Tijing, L. D.; Ruelo, M. T. G.; Lee, D. H.; Kim, C. S. Facile synthesis and immobilization of Ag−TiO₂ nanoparticles on electrospun PU nanofibers by polyol technique and simple immersion. *Mater. Chem. Phys.* **2012**, *135* (2−3), 277−281.

(13) Pant, H. R.; Pandeya, D. R.; Nam, K. T.; Baek, W.-I.; Hong, S. T.; Kim, H. Y. Photocatalytic and antibacterial properties of a TiO₂/nylon-6 electrospun nanocomposite mat containing silver nanoparticles. *J. Hazard. Mater.* **2011**, *189* (1−2), 465−471.

(14) Kim, S. H.; Kwak, S.-Y.; Sohn, B.-H.; Park, T. H. Design of TiO₂ nanoparticle self-assembled aromatic polyamide thin-film-composite (TFC) membrane as an approach to solve biofouling problem. *J. Membr. Sci.* **2003**, *211* (2), 157−165.

(15) Tang, Z.; Kotov, N. A.; Magonov, S.; Ozturk, B. Nanostructured artificial nacre. *Nat. Mater.* **2003**, *2* (6), 413−418.

(16) Podsiadlo, P.; Paternel, S.; Rouillard, J. M.; Zhang, Z.; Lee, J.; Lee, J. W.; Gulari, E.; Kotov, N. A. Layer-by-layer assembly of nacre-like nanostructured composites with antimicrobial properties. *Langmuir* **2005**, *21* (25), 11915−11921.

(17) Elzatahry, A. A.; Al-Enizi, A. M.; Elsayed, E. A.; Butorac, R. R.; Al-Deyab, S. S.; Wadaan, M. A.; Cowley, A. H. Nanofiber composites containing N-heterocyclic carbene complexes with antimicrobial activity. *Int. J. Nanomed.* **2012**, *7*, 2829−2832.

(18) Xing, Z.-C.; Meng, W.; Yuan, J.; Moon, S.; Jeong, Y.; Kang, I.-K. In vitro assessment of antibacterial activity and cytocompatibility of quercetin-containing PLGA nanofibrous scaffolds for tissue engineering. *J. Nanomater.* **2012**, *2012*, 1.

(19) Genzer, J.; Efimenko, K. Recent developments in super-hydrophobic surfaces and their relevance to marine fouling: A review. *Biofouling* **2006**, *22*, 339−360.

(20) Park, K. D.; Kim, Y. S.; Han, D. K.; Kim, Y. H.; Lee, E. H. B.; Suh, H.; Choi, K. S. Bacterial adhesion on PEG modified polyurethane surfaces. *Biomaterials* **1998**, *19* (7−9), 851−859.

(21) Ostuni, E.; Chapman, R. G.; Liang, M. N.; Meluleni, G.; Pier, G.; Ingber, D. E.; Whitesides, G. M. Self-assembled monolayers that

1004

dx.doi.org/10.1021/sc400564r | *ACS Sustainable Chem. Eng.* 2014, 2, 996−1006

resist the adsorption of proteins and the adhesion of bacterial and mammalian cells. *Langmuir* **2001**, *17* (20), 6336−6343.

(22) Li, L.; Chen, S.; Jiang, S. Protein interactions with oligo-(ethylene glycol) (OEG) self-assembled monolayers: OEG stability, surface packing density and protein adsorption. *J. Biomater. Sci., Polym. Ed.* **2007**, *18* (11), 1415−1427.

(23) Ostuni, E.; Chapman, R. G.; Holmlin, R. E.; Takayama, S.; Whitesides, G. M. A survey of structure−property relationships of surfaces that resist the adsorption of protein. *Langmuir* **2001**, *17* (18), 5605−5620.

(24) Schmitt, M. A.; Weisblum, B.; Gellman, S. H. Unexpected relationships between structure and function in α,β-peptides: Antimicrobial foldamers with heterogeneous backbones. *J. Am. Chem. Soc.* **2004**, *126* (22), 6848−6849.

(25) Schmitt, M. A.; Weisblum, B.; Gellman, S. H. Interplay among folding, sequence, and lipophilicity in the antibacterial and hemolytic activities of α/β-peptides. *J. Am. Chem. Soc.* **2007**, *129* (2), 417−428.

(26) Feiertag, P.; Albert, M.; Ecker-Eckhofen, E.-M.; Hayn, G.; Hönig, H.; Oberwalder, H. W.; Saf, R.; Schmidt, A.; Schmidt, O.; Topchiev, D. Structural characterization of biocidal oligoguanidines. *Macromol. Rapid Commun.* **2003**, *24* (9), 567−570.

(27) Albert, M.; Feiertag, P.; Hayn, G.; Saf, R.; Hönig, H. Structure−activity relationships of oligoguanidinesinfluence of counterion, diamine, and average molecular weight on biocidal activities. *Biomacromolecules* **2003**, *4* (6), 1811−1817.

(28) Kenawy, E. R.; Mahmoud, Y. A. G. Biologically active polymers. *Macromol. Biosci.* **2003**, *3* (2), 107−115.

(29) Kenawy, E.-R.; Abdel-Hay, F. I.; El-Magd, A. A.; Mahmoud, Y. A. G. Biologically active polymers: VII. Synthesis and antimicrobial activity of some crosslinked copolymers with quaternary ammonium and phosphonium groups. *React. Funct. Polym.* **2006**, *66* (4), 419−429.

(30) Chang, Y.; Yandi, W.; Chen, W. Y.; Shih, Y. J.; Yang, C. C.; Ling, Q. D.; Higuchi, A. Tunable bioadhesive copolymer hydrogels of thermoresponsive poly(N-isopropyl acrylamide) containing zwitterionic polysulfobetaine. *Biomacromolecules* **2010**, *11* (4), 1101−1110.

(31) Chang, Y.; Liao, S.-C.; Higuchi, A.; Ruaan, R.-C.; Chu, C.-W.; Chen, W.-Y. A highly stable nonbiofouling surface with well-packed grafted zwitterionic polysulfobetaine for plasma protein repulsion. *Langmuir* **2008**, *24* (10), 5453−5458.

(32) Iemma, F.; Puoci, F.; Curcio, M.; Parisi, O. I.; Cirillo, G.; Spizzirri, U. G.; Picci, N. Ferulic acid as a comonomer in the synthesis of a novel polymeric chain with biological properties. *J. Appl. Polym. Sci.* **2010**, *115* (2), 784−789.

(33) Herold, B. C.; Scordi-Bello, I.; Cheshenko, N.; Marcellino, D.; Dzuzelewski, M.; Francois, F.; Morin, R.; Casullo, V. M.; Anderson, R. A.; Chany, C. I.; Waller, D. P.; Zaneveld, L. J. D.; Klotman, M. E. Mandelic acid condensation polymer: Novel candidate microbicide for prevention of human immunodeficiency virus and herpes simplex virus entry. *J. Virol.* **2002**, *76* (22), 11236−11244.

(34) Al-Muaikel, N. S.; Al-Diab, S. S.; Al-Salamah, A. A.; Zaid, A. M. A. Synthesis and characterization of novel organotin monomers and copolymers and their antibacterial activity. *J. Appl. Polym. Sci.* **2000**, *77* (4), 740−745.

(35) Lichter, J. A.; Van Vliet, K. J.; Rubner, M. F. Design of antibacterial surfaces and interfaces: Polyelectrolyte multilayers as a multifunctional platform. *Macromolecules* **2009**, *42* (22), 8573−8586.

(36) Ignatova, M.; Starbova, K.; Markova, N.; Manolova, N.; Rashkov, I. Electrospun nano-fibre mats with antibacterial properties from quaternised chitosan and poly(vinyl alcohol). *Carbohydr. Res.* **2006**, *341* (12), 2098−2107.

(37) Ignatova, M.; Manolova, N.; Rashkov, I. Novel antibacterial fibers of quaternized chitosan and poly(vinylpyrrolidone) prepared by electrospinning. *Eur. Polym. J.* **2007**, *43* (4), 1112−1122.

(38) Ignatova, M.; Petkova, Z.; Manolova, N.; Markova, N.; Rashkov, I. Non-woven fibrous materials with antibacterial properties prepared by tailored attachment of quaternized chitosan to electrospun mats from maleic anhydride copolymer. *Macromol. Biosci* **2012**, *12* (1), 104−115.

(39) El Habnouni, S.; Darcos, V.; Garric, X.; Lavigne, J.-P.; Nottelet, B.; Coudane, J. Mild methodology for the versatile chemical modification of polylactide surfaces: Original combination of anionic and click chemistry for biomedical applications. *Adv. Funct. Mater.* **2011**, *21* (17), 3321−3330.

(40) Cheng, G.; Zhang, Z.; Chen, S. F.; Bryers, J. D.; Jiang, S. Y. Inhibition of bacterial adhesion and biofilm formation on zwitterionic surfaces. *Biomaterials* **2007**, *28* (29), 4192−4199.

(41) Yang, W.; Chen, S.; Cheng, G.; Vaisocherová, H.; Xue, H.; Li, W.; Zhang, J.; Jiang, S. Film thickness dependence of protein adsorption from blood serum and plasma onto poly(sulfobetaine)-grafted surfaces. *Langmuir* **2008**, *24* (17), 9211−9214.

(42) Sakuragi, M.; Tsuzuki, S.; Obuse, S.; Wada, A.; Matoba, K.; Kubo, I.; Ito, Y. A photoimmobilizable sulfobetaine-based polymer for a nonbiofouling surface. *Mater. Sci. Eng: C* **2010**, *30* (2), 316−322.

(43) Lin, J.; Tiller, J.; Lee, S.; Lewis, K.; Klibanov, A. Insights into bactericidal action of surface-attached poly(vinyl-N-hexylpyridinium) chains. *Biotechnol. Lett.* **2002**, *24* (10), 801−805.

(44) Jon, S.; Seong, J.; Khademhosseini, A.; Tran, T.-N. T.; Laibinis, P. E.; Langer, R. Construction of nonbiofouling surfaces by polymeric self-assembled monolayers. *Langmuir* **2003**, *19* (24), 9989−9993.

(45) Ye, S.-H.; Johnson, C. A., Jr; Woolley, J. R.; Murata, H.; Gamble, L. J.; Ishihara, K.; Wagner, W. R. Simple surface modification of a titanium alloy with silanated zwitterionic phosphorylcholine or sulfobetaine modifiers to reduce thrombogenicity. *Colloids Surf., B* **2010**, *79* (2), 357−364.

(46) Tiller, J. C.; Lee, S. B.; Lewis, K.; Klibanov, A. M. Polymer surfaces derivatized with poly(vinyl-N-hexylpyridinium) kill airborne and waterborne bacteria. *Biotechnol. Bioeng.* **2002**, *79* (4), 465−471.

(47) Lee, S. B.; Koepsel, R. R.; Morley, S. W.; Matyjaszewski, K.; Sun, Y.; Russell, A. J. Permanent, nonleaching antibacterial surfaces. 1. Synthesis by atom transfer radical polymerization. *Biomacromolecules* **2004**, *5* (3), 877−882.

(48) Hazer, D. B.; Kiliçay, E.; Hazer, B. Poly(3-hydroxyalkanoate)s: Diversification and biomedical applications: A state of the art review. *Mater. Sci. Eng., C* **2012**, *32* (4), 637−647.

(49) Steinbüchel, A.; Valentin, H. E. Diversity of bacterial polyhydroxyalkanoic acids. *FEMS Microbiol. Lett.* **1995**, *128* (3), 219−228.

(50) Sudesh, K.; Abe, H.; Doi, Y. Synthesis, structure and properties of polyhydroxyalkanoates: biological polyesters. *Prog. Polym. Sci.* **2000**, *25* (10), 1503−1555.

(51) Versace, D.-L.; Ramier, J.; Babinot, J.; Lemechko, P.; Soppera, O.; Lalevee, J.; Albanese, P.; Renard, E.; Langlois, V. Photoinduced modification of the natural biopolymer poly(3-hydroxybutyrate-co-3-hydroxyvalerate) microfibrous surface with anthraquinone-derived dextran for biological applications. *J. Mater. Chem. B* **2013**, *1* (37), 4834−4844.

(52) Versace, D.-L.; Ramier, J.; Grande, D.; Andaloussi, S. A.; Dubot, P.; Hobeika, N.; Malval, J.-P.; Lalevee, J.; Renard, E.; Langlois, V. Versatile photochemical surface modification of biopolyester micro-fibrous scaffolds with photogenerated silver nanoparticles for antibacterial activity. *Adv. Healthcare Mater.* **2013**, *2* (7), 1008−1018.

(53) Chen, G.-Q.; Wu, Q. The application of polyhydroxyalkanoates as tissue engineering materials. *Biomaterials* **2005**, *26* (33), 6565−6578.

(54) Schakenraad, J. M.; Oosterbaan, J. A.; Nieuwenhuis, P.; Molenaar, I.; Olijslager, J.; Potman, W.; Eenink, M. J. D.; Feijen, J. Biodegradable hollow fibres for the controlled release of drugs. *Biomaterials* **1988**, *9* (1), 116−120.

(55) Misra, S. K.; Valappil, S. P.; Roy, I.; Boccaccini, A. R. Polyhydroxyalkanoate (PHA)/inorganic phase composites for tissue engineering applications. *Biomacromolecules* **2006**, *7* (8), 2249−2258.

(56) Wang, Y.-W.; Yang, F.; Wu, Q.; Cheng, Y.-c.; Yu, P. H. F.; Chen, J.; Chen, G.-Q. Effect of composition of poly(3-hydroxybutyrate-co-3-hydroxyhexanoate) on growth of fibroblast and osteoblast. *Biomaterials* **2005**, *26* (7), 755−761.

(57) Babinot, J.; Guigner, J.-M.; Renard, E.; Langlois, V. Poly(3-hydroxyalkanoate)-derived amphiphilic graft copolymers for the design of polymersomes. *Chem. Commun.* **2012**, *48* (43), 5364−5366.

(58) Babinot, J.; Guigner, J.-M.; Renard, E.; Langlois, V. A micellization study of medium chain length poly(3-hydroxyalkanoate)-based amphiphilic diblock copolymers. *J. Colloid Interface Sci.* **2012**, *375* (1), 88−93.

(59) Linhart, W.; Lehmann, W.; Siedler, M.; Peters, F.; Schilling, A.; Schwarz, K.; Amling, M.; Rueger, J.; Epple, M. Composites of amorphous calcium phosphate and poly(hydroxybutyrate) and poly(hydroxybutyrate-co-hydroxyvalerate) for bone substitution: assessment of the biocompatibility. *J. Mater. Sci.* **2006**, *41* (15), 4806−4813.

(60) Ying, T. H.; Ishii, D.; Mahara, A.; Murakami, S.; Yamaoka, T.; Sudesh, K.; Samian, R.; Fujita, M.; Maeda, M.; Iwata, T. Scaffolds from electrospun polyhydroxyalkanoate copolymers: Fabrication, characterization, bioabsorption and tissue response. *Biomaterials* **2008**, *29* (10), 1307−1317.

(61) Cheng, M.-L.; Chen, P.-Y.; Lan, C.-H.; Sun, Y.-M. Structure, mechanical properties and degradation behaviors of the electrospun fibrous blends of PHBHHx/PDLLA. *Polymer* **2011**, *52* (6), 1391−1401.

(62) Li, X.; Liu, K. L.; Wang, M.; Wong, S. Y.; Tjiu, W. C.; He, C. B.; Goh, S. H.; Li, J. Improving hydrophilicity, mechanical properties and biocompatibility of poly[(R)-3-hydroxybutyrate-co-(R)-3-hydroxyvalerate] through blending with poly[(R)-3-hydroxybutyrate]-alt-poly(ethylene oxide). *Acta Biomater.* **2009**, *5* (6), 2002−2012.

(63) Wang, Y.-Y.; Lü, L.-X.; Shi, J.-C.; Wang, H.-F.; Xiao, Z.-D.; Huang, N.-P. Introducing RGD peptides on PHBV films through PEG-containing cross-linkers to improve the biocompatibility. *Biomacromolecules* **2011**, *12* (3), 551−559.

(64) Grøndahl, L.; Chandler-Temple, A.; Trau, M. Polymeric grafting of acrylic acid onto poly(3-hydroxybutyrate-co-3-hydroxyvalerate): Surface functionalization for tissue engineering applications. *Biomacromolecules* **2005**, *6* (4), 2197−2203.

(65) Lao, H.-K.; Renard, E.; Linossier, I.; Langlois, V.; Vallée-Rehel, K. Modification of poly(3-hydroxybutyrate-co-3-hydroxyvalerate) film by chemical graft copolymerization. *Biomacromolecules* **2006**, *8* (2), 416−423.

(66) Versace, D.-L.; Dubot, P.; Cenedese, P.; Lalevee, J.; Soppera, O.; Malval, J.-P.; Renard, E.; Langlois, V. Natural biopolymer surface of poly(3-hydroxybutyrate-co-3-hydroxyvalerate)-photoinduced modification with triarylsulfonium salts. *Green Chem.* **2012**, *14* (3), 788−798.

(67) Fouassier, J.-P.; Rabek, J. F. *Radiation Curing in Polymer Science and Technology*; Elsevier Applied Science: London, 1993.

(68) Fouassier, J. P.; Lalevée, J. *Photoinitiators for Polymer Synthesis: Scope, Reactivity, and Efficiency*; Wiley: New York, 2013.

(69) Lao, H.-K.; Renard, E.; Fagui, A. E.; Langlois, V.; Vallée-Rehel, K.; Linossier, I. Functionalization of poly(3-hydroxybutyrate-co-3-hydroxyvalerate) films via surface-initiated atom transfer radical polymerization: Comparison with the conventional free-radical grafting procedure. *J. Appl. Polym. Sci.* **2011**, *120* (1), 184−194.

(70) Ma, H.; Davis, R. H.; Bowman, C. N.; Novel, A. Sequential photoinduced living graft polymerization. *Macromolecules* **2000**, *33* (2), 331−335.

(71) Ke, Y.; Wang, Y.; Ren, L.; Lu, L.; Wu, G.; Chen, X.; Chen, J. Photografting polymerization of polyacrylamide on PHBV films (I). *J. Appl. Polym. Sci.* **2007**, *104* (6), 4088−4095.

(72) Rupp, B.; Ebner, C.; Rossegger, E.; Slugovc, C.; Stelzer, F.; Wiesbrock, F. UV-induced crosslinking of the biopolyester poly(3-hydroxybutyrate)-co-(3-hydroxyvalerate). *Green Chem.* **2010**, *12* (10), 1796−1802.

(73) Lao, H.-K.; Renard, E.; Langlois, V.; Vallée-Rehel, K.; Linossier, I. Surface functionalization of PHBV by HEMA grafting via UV treatment: Comparison with thermal free radical polymerization. *J. Appl. Polym. Sci.* **2010**, *116* (1), 288−297.

(74) Janzen, E. G.; Lopp, I. G.; Morgan, T. V. Detection of fluoroalkyl and acyl radicals in the gas-phase photolysis of ketones and aldehydes by electron spin resonance gas-phase spin trapping techniques. *J. Phys. Chem.* **1973**, *77* (1), 139−141.

(75) Knoll, H. Methyl radical addition to methyl ethyl ketone. *React. Kinet. Catal. Lett.* **1981**, *15* (4), 431−435.

(76) Wang, H.; Brown, H. R. Ultraviolet grafting of methacrylic acid and acrylic acid on high-density polyethylene in different solvents and the wettability of grafted high-density polyethylene. I. Grafting. *J. Polym. Sci., Part A: Polym. Chem* **2004**, *42* (2), 253−262.

(77) Muñoz-Bonilla, A.; Fernández-García, M. Polymeric materials with antimicrobial activity. *Prog. Polym. Sci.* **2012**, *37* (2), 281−339.

(78) Gottenbos, B.; Grijpma, D. W.; van der Mei, H. C.; Feijen, J.; Busscher, H. J. Antimicrobial effects of positively charged surfaces on adhering Gram-positive and Gram-negative bacteria. *J. Antimicrob. Chemother.* **2001**, *48* (1), 7−13.

(79) Zhao, T.; Sun, G. Hydrophobicity and antimicrobial activities of quaternary pyridinium salts. *J. Appl. Microbiol.* **2008**, *104* (3), 824−830.